Theor Appl Climatol (2010) 102:367–378
DOI 10.1007/s00704-010-0259-x

ORIGINAL PAPER

Flood-producing cloud bands over the Kalahari Desert

Mark R. Jury

Received: 19 August 2009 / Accepted: 10 January 2010 / Published online: 5 March 2010

Abstract The characteristics of flood-producing cloud bands over the Kalahari Desert (15-30°S, 15-22°E) are described using daily time-scale observations, reanalysis and satellite data. The cloud band extends southward from Angola, producing short periods of intense rainfall over Namibia. Their frequency of occurrence is ~8% according to singular value decomposition of gridded 1° daily GPCP rainfall 1996-2008. The environmental features evident from case study and composite analysis include: (1) cut-off low over the Namibian coast and deep anticyclonic ridge south of Africa, (2) inflow of air from vegetated surfaces to the northeast ($Q>300$ W m^{-2}) into a 300 km wide meridional axis, (3) a large-scale sea breeze that enhances afternoon convection, and in the background, (4) warming of the southeast Atlantic Ocean off Angola. Short-range GFS forecasts appear accurate for the devastating 5 February 2009 event 5 days in advance.

1 Introduction

Deep convection over Central Africa acts as a driver of the global circulation and research has characterized its oscillations and links with Atlantic sea surface temperatures (SST) and the climate of West, East, and Southern Africa (Hirst and Hastenrath 1983; Laing and Fritsch 1993; Jury and Engert 1999; Jury et al. 2000; Camberlin et al. 2001; Rouault et al. 2003; Todd and Washington 2004; Jury et al. 2008). Some studies have characterized intra-seasonal oscillations over Central Africa (Mutai and Ward 2000; Tazalika and Jury 2008), yet our understanding of its effects on the surrounding weather is limited. McCollum et al. (2000) studied the cloud properties of Central Africa and determined the convection to be vigorous but inefficient due to loading by desert dust with particle sizes 10-20 μm. Using the Tropical Rainfall Measuring Mission (TRMM) satellite data, Zipser (2003) found that Central Africa is the only equatorial zone where lightning, and thus deep convection in ice phase, is frequent year-round. Convective outflows can spread towards northern and southern Africa, but little is known of processes by which this occurs.

The Kalahari Desert region (Fig. 1a,b) extending from 15-30°S, 15-22°E, receives little rainfall due to tropospheric subsidence and divergent equatorward air flowing next to the cold Benguela current. Convection can be generated by a particular weather feature known as a cut-off low. These deep cold-cored lows originate in the mid-latitude westerlies and can migrate equatorward during jet stream loops (Taljaard 1985, 1994) when a mid-latitude ridge undercuts a sub-tropical low. Such lows drift slowly in the sub-tropics and may interact with tropical air masses over Central Africa. Infrequently, during austral summer (November to April), meridional cloud bands may link cut-off lows over South Africa with a tropical vortex in the western Zambezi Valley (15°S, 15-25°E, Fig. 1a) bringing rains to the Kalahari.

In the austral summer of 2009 over 400,000 people were affected by flooding in Namibia. Impacts included 90,000 ha of land and 25,000 homes washed away, 125,000 people displaced and ~100 deaths. Hydrologists reported the 2009 floods to be the worst in 35 years. Two hundred fifty thousand people were cut-off from road transport and many were evacuated as the Kwando River

M. R. Jury
University of Zululand,
KwaDlangezwa, South Africa 3886

M. R. Jury (✉)
Physics Department, University of Puerto Rico Mayagüez,
Mayagüez 00681, Puerto Rico
e-mail: mark.jury@upr.edu

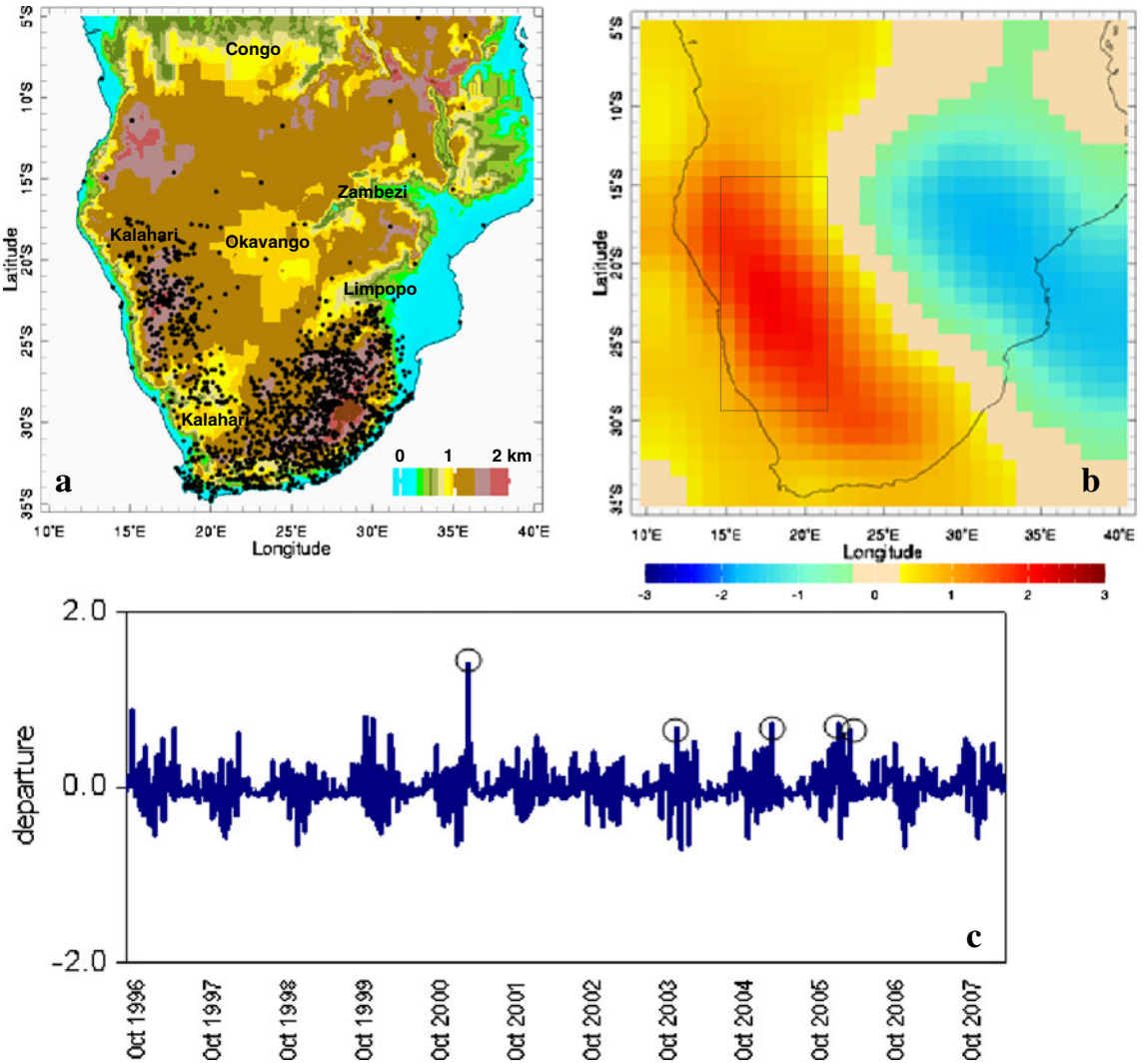

Fig. 1 **a** Topographic map of southern Africa with daily reporting stations and place names, **b** GPCP mode-2 rainfall SVD loading, and **c** time score. *Shading* in **b** scaled according to color bar with sigma units. *Box* **b** outlines Kalahari area; case studies are identified by circles in **c**

feeding the Okavango Delta reached its highest level since 1939. Over 50 flood-related deaths were recorded in Angola and Zambia. Floods swept away livestock and crops, causing food shortages and outbreaks of cholera and malaria. Infrastructure already vulnerable from earlier flooding collapsed, stretching national disaster management capacity similar to the floods of 1988 (Triegaardt et al. 1991; Alexander and van Heerden 1991) and 2000 (Dyson and van Heerden 2001).

Given these impacts, this paper investigates meridional cloud bands over the Kalahari in austral summer and the regional atmospheric circulation and thermodynamic patterns that surround major flood events. The backdrop for these events is studied to understand links between weather and ocean climate, as in Muller et al. (2007). The physical structure and mechanisms are analyzed and a number of questions are addressed: (1) is rainfall over the Kalahari related to a specific circulation pattern? (2) Which meteorological features are most important and how often do they occur? (3) How significant is the diurnal cycle and what are its characteristics? (4) What is the role of ocean anomalies in Kalahari flood events? In section 2 the data and methods are outlined. Section 3 provides results by analysis of daily rainfall, investigation of peak events, and inter-relationships with the regional meteorology. A seasonal context is provided using ocean reanalysis data, whilst conclusions are given in Section 4.

2 Data and methods

To establish the nature of rain events over the Kalahari, univariate singular value decomposition (SVD) is applied to daily satellite-gauge merged data over the period 1996-2008. The primary rainfall data derive from the Global Precipitation Climatology Project (GPCP) of the World

Climate Research Program, whereby all reported gauge data (Fig. 1a) is interpolated to a 1.0° grid using the pattern of multi-satellite brightness temperatures (Huffman et al. 2001) involving polar and geostationary satellites and microwave and infrared radiometers. A second rainfall product originating from the Famine Early Warning System (FEWS) for Africa is also employed that uses a different blending of gauges and multiple satellite radiometers to a nominal 0.5° resolution (Herman et al. 1997; Love et al. 2004). Daily rainfall time series are filtered to 3-day averages to rank flood events. Histograms are analyzed for rainfall and a weather index to establish the frequency of occurrence. The weather index is formulated by subtracting standardized departures of 500 hPa geopotential heights at 35-40ºS from 20-25ºS, then adding precipitable water 20-25ºS, all in the longitudes 10-25°E. This focuses on a certain weather scenario wherein tropical moisture is drawn toward the Kalahari by a mid-latitude ridge and sub-tropical cut-off low, as outlined by Singleton and Reason (2007).

The SVD analysis involves an eigenvector decomposition of the covariance matrix within a single input field (similar to empirical orthogonal functions), such that the variability is reduced to modes in order of decreasing explained variance normalized to a total of one. For each unique mode, there is a spatial pattern of weights or loadings and a series of expansion coefficients or time scores that describe its temporal fluctuations, both with units of standard deviations relative to each mode (Bretherton et al. 1992). SVD time scores are used in cross-correlation, multi-variate regression and scatterplot analysis. The goal here is to uncover the pattern of daily rainfall over Southern Africa in the period 1996-2008, then to understand the forcing of major events by subsequent examination of meteorological variables. The first mode of variability that emerges from SVD analysis is a zonal cluster over the Zambezi Valley, while the second mode is a NW-oriented cluster over the Kalahari with inverse loading over Mozambique (dipole). As will be seen later, this east-west

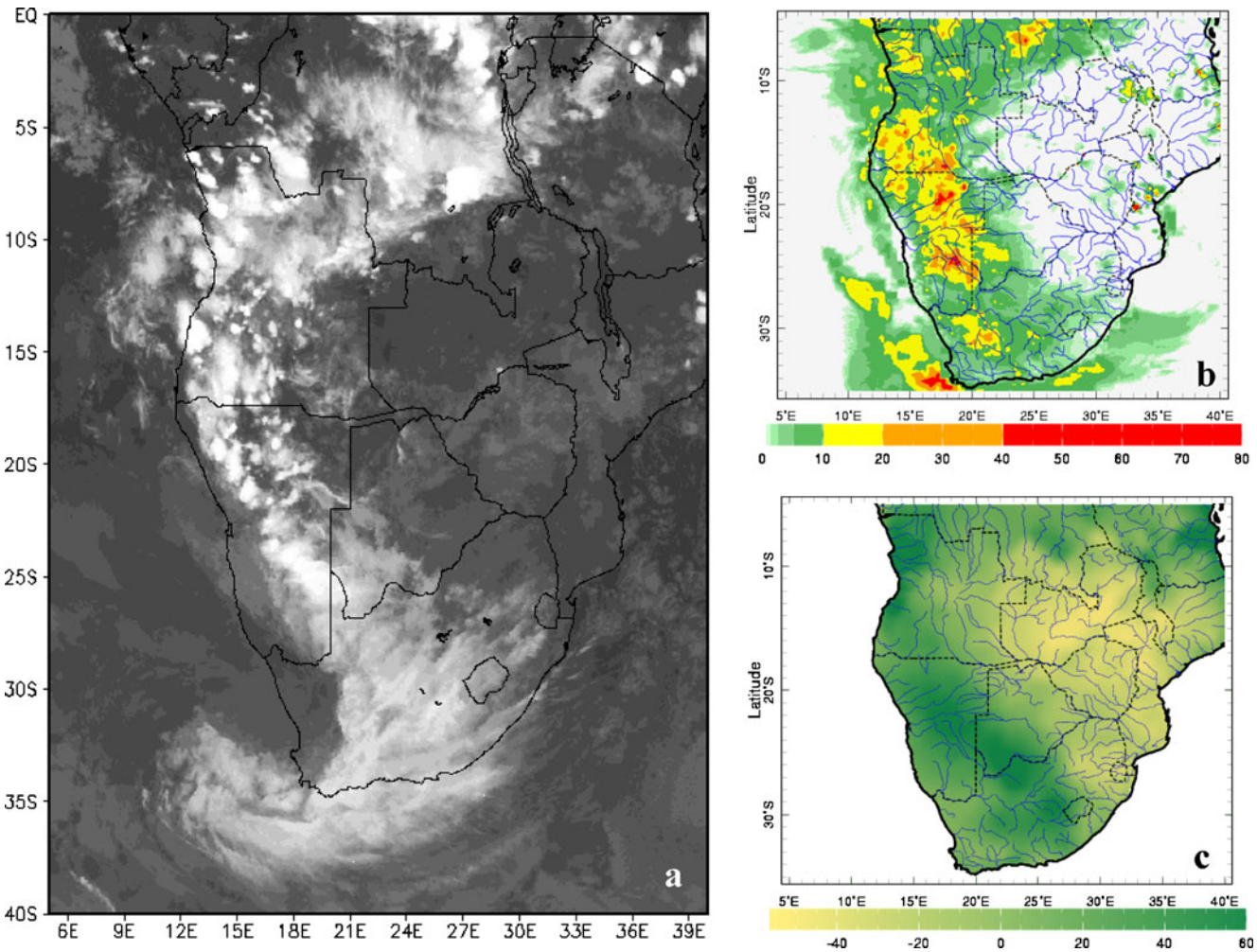

Fig. 2 **a** Meteosat IR image 1600 LST 6 April 2001 with S-shaped cloud band, **b** FEWS rainfall map for 5-7 April 2001, **c** CPC soil moisture difference from March to April 2001 (mm) with rivers plotted

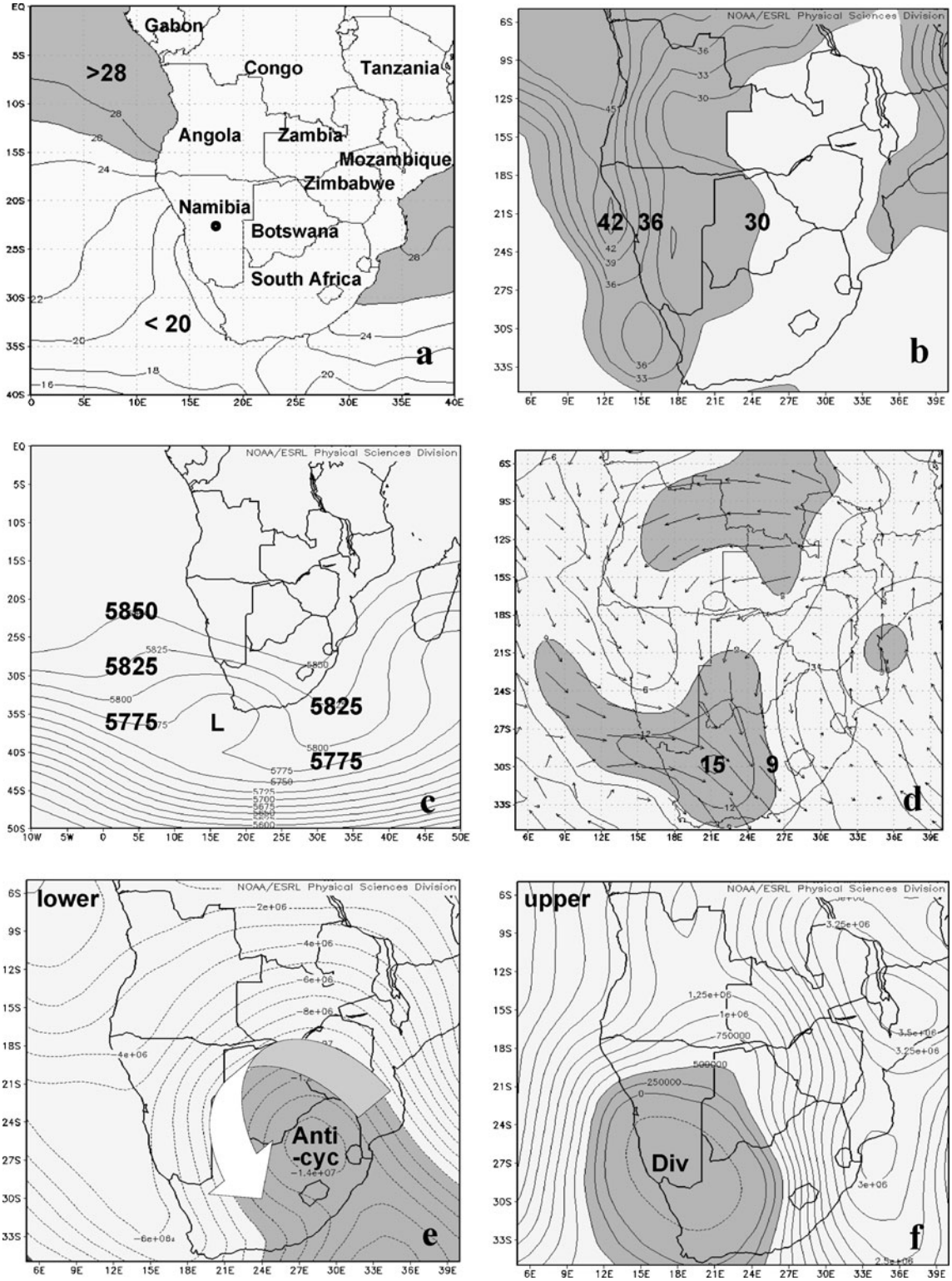

Fig. 3 Composite mean maps for 5-7 April 2001: **a** NOAA SST, **b** NCEP precipitable water, **c** 500 hPa geopotential height, **d** 700 hPa vector wind, **e** NCEP 850 hPa stream function, and **f** NCEP 250 hPa velocity potential. Country names are given in **a**, *dot* is Windhoek

alternation is underpinned by meteorological forcing and is not an artifact.

From a ranking of GPCP and FEWS SVD mode-2 time scores, a peak event: 5-7 April 2001 and a group of four strong events: 5-7 January 2004, 5-7 April 2005, 23-25 February 2006, and 15-17 April 2006 are selected for analysis. This last event was studied by Muller et al. (2007) wherein a cut-off low and favorable SST patterns were

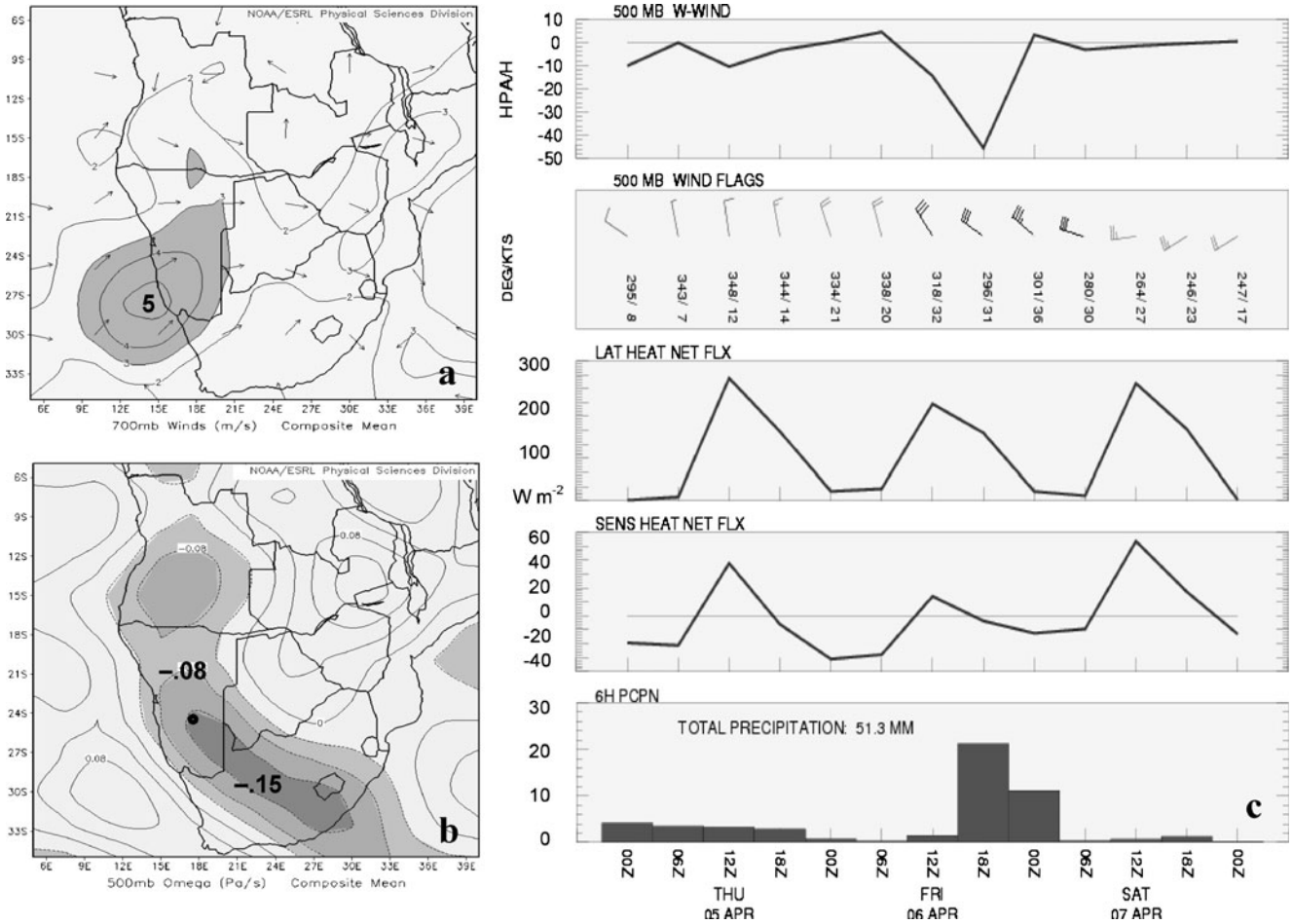

Fig. 4 Diurnal cycle amplitude for 5-7 April 2001 case: **a** 700 hPa wind (m s^{-1}) and **b** 500 hPa omega (Pa s^{-1}) difference from 02-08 LST to 14-20 LST, and **c** time series of GFS analysis for 25°S,18°E (*dot* in **b**)

found. The meteorological scenario is studied via National Center for Environmental Prediction (NCEP) reanalysis (Kalnay et al. 1996) and National Oceanic and Atmospheric Administration (NOAA) satellite data (Smith and Reynolds 2004) as in the past studies (e. g., Todd and Washington 2004). The regional setting for sea surface temperature, geopotential height, winds, vertical motion, precipitable water, and the divergent and rotational circulation is analyzed. For the peak flood event in 2001, total fields are mapped, whereas for the group of four cases in 2004-2006, a composite average is calculated and the historical mean is subtracted to produce anomaly maps and vertical sections. The amplitude of diurnal forcing is studied by subtracting fields for 0200-0800 Local Standard Time (LST) from 1400-2000 LST. Reanalysis products are supplemented by Windhoek (23°S, 18°E) radiosonde profiles and satellite data from Meteosat, TRMM, and MODIS. There are few surface observations in the northern Kalahari other than daily rain gauges.

While methods to reveal the meteorological forcing have been discussed, the oceanographic conditions may provide some influence. To determine this, monthly Simple Ocean Data Assimilation fields (SODA 2.4, Carton and Giese 2008) comprising ECMWF wind stress, sea surface height, temperature, currents, and salinity are analyzed. Although SSTs off Angola are above normal during Kalahari cloud band events, not all southeast Atlantic warm events enhance seasonal rainfall. So to select cases for analysis, an objective two-tier approach is used that ranks the Angola SST and then ranks the Kalahari rainfall. Months with warm Angola SST and wet Kalahari weather include February-March of 1968, 1976, 1977, 1989, 2000, 2001, and 2006. The composite fields are averaged and the historical mean is subtracted, so ocean anomalies are evaluated for the tropical southeast Atlantic and Angola shelf zone.

3 Results

3.1 A rainfall mode over the Kalahari

The leading mode of daily GPCP rainfall in the 1996-2008 period is a zonal feature over the Zambezi with an annual

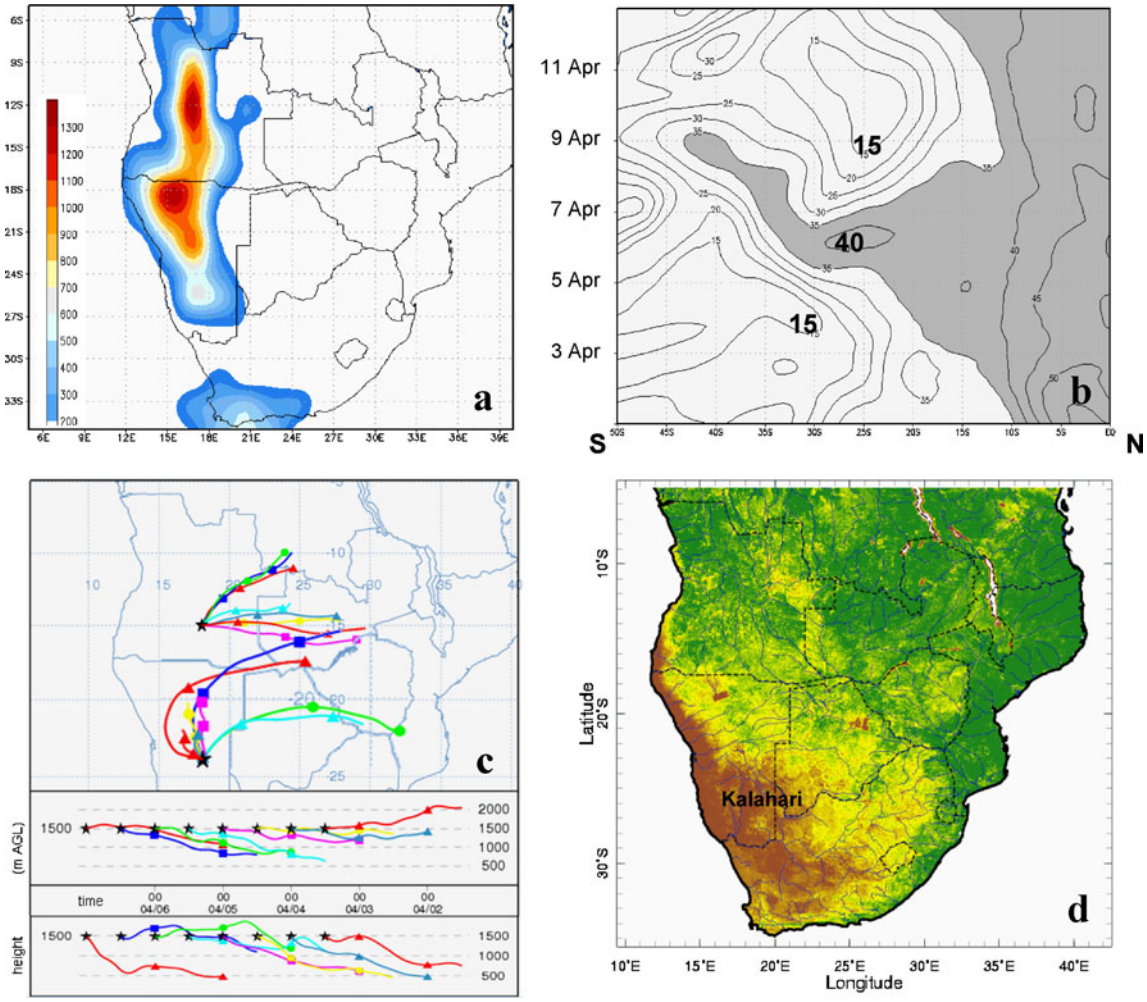

Fig. 5 **a** NCEP cloud work function for 6 April and **b** hovmoller time-longitude plot of precipitable water for 1-12 April 2001 along 15-20°E slice, **c** Hysplit back-trajectories for 2-6 April 2001 in *plan* and *vertical section* and **d** satellite vegetation index for 1-15 April 2001 with NDVI colors from 0.1 *brown* to 0.7 *green*

cycle that peaks in January as the inter-tropical trough migrates southward following the sun angle. This zonal mode has been documented (Jury and Mpeta 2009) and is not the focus here. The second mode of daily rainfall variability is represented as a west (positive)—east (negative) dipole (Fig. 1b). It shows maximum fluctuation in austral summer as expected (Fig. 1c). This meridional mode explains 8% of variance whereas the leading zonal mode has 27%. The positive loaded area lies over the Kalahari, and coincides with negative loading over southeastern Africa. Its orientation is consistent with NW cloud bands that are the main source of intra-seasonal rainfall variability over southern Africa (Harrison 1988; Crimp et al. 1997) and related to the position of large-scale atmospheric Rossby waves in the sub-tropical jet stream (Lindesay and Jury 1991; Karoly and Vincent 1998). The mode-2 time score provides a useful measure of the strength of Kalahari cloud bands. In negative phase, rains shift to Mozambique. Objectively ranking the 3-day Kalahari rainfall, it is found that the 5-7 April 2001 event exceeds others, while a group of four cases: 5-7 January 2004, 5-7 April 2005, 23-25 February 2006, and 15-17 April 2006 are in the next tier of event strength. The latter case was studied by Muller et al. (2007). Histogram analysis reveals that 6.6% of the time the Kalahari area-averaged rainfall (15-30°S, 15-22°E) exceeds 5 mm/day, while the weather index indicating a moist cut-off low occurs 11.6% of the time.

3.2 Case study of 5-7 April 2001

In this section, the regional meteorological scenario surrounding a peak Kalahari cloud band event of 5-7 April 2001 is analyzed using mean maps. The IR satelllite image for 6 April 2001 indicates the cloud band has an ‘S’ shape (Fig. 2a), whilst the FEWS rainfall field in Fig. 2b illustrates a broad NW-SE swath of 20-40 mm across Namibia, southern Angola and western South Africa. The CPC soil moisture difference from March and April 2001

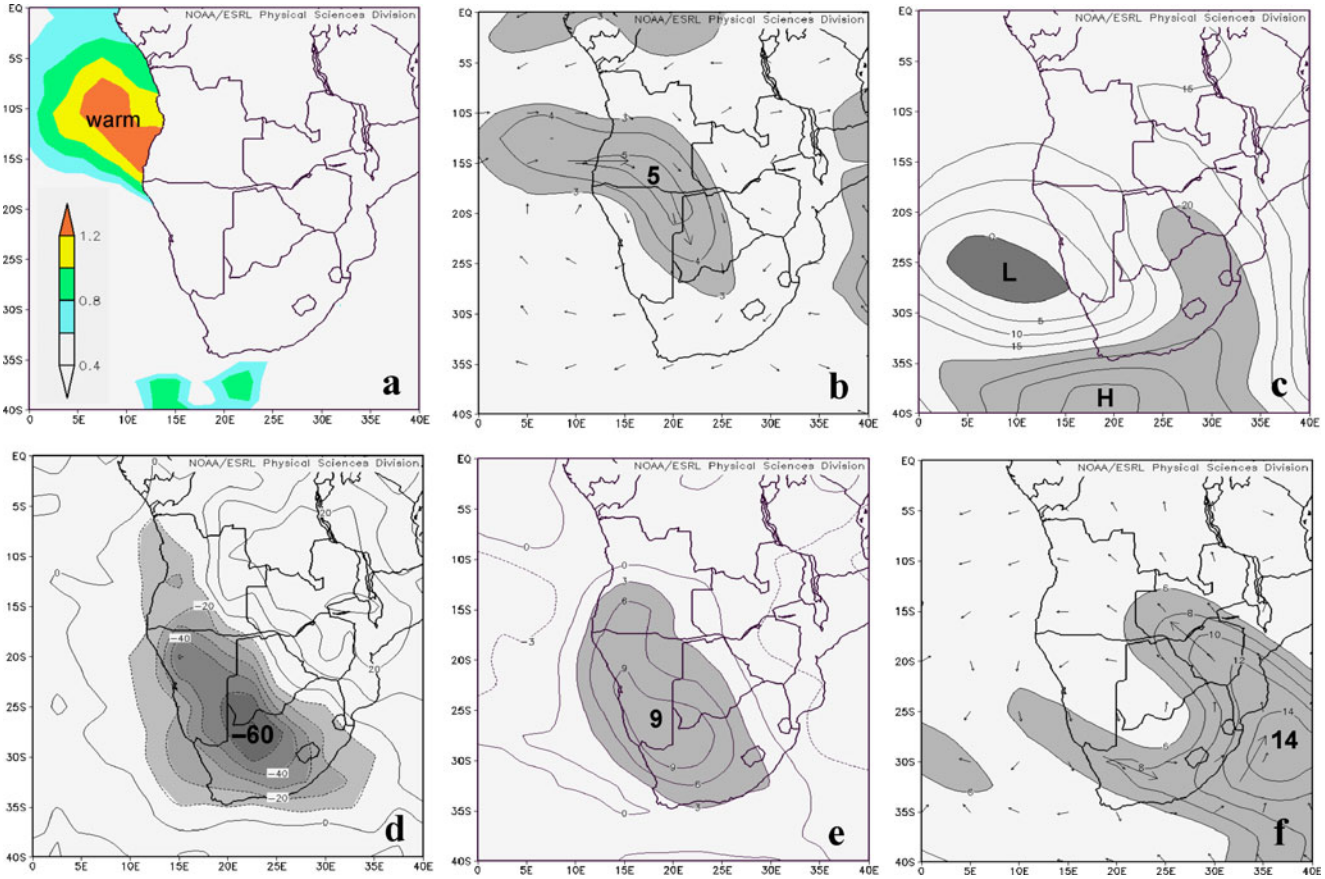

Fig. 6 Composite anomaly fields of four peak cases in the 2004-2006 summers (*top* **a**, **b**, **c**) SST (C), 700 hPa wind, 500 hPa geopotential height (m; *lower* **d**,**e**,**f**) satellite OLR (W m^{-2}), NCEP precipitable water (mm) and 200 hPa wind (m s^{-1})

exceeded 40 mm over a similar zone (Fig. 2c). Rainfall records indicate that this event was rather isolated. The scenario is analyzed in detail in Fig. 3a-f. SST were >28°C over a broad area off Angola during the first week in April (+2°C anomaly). In response to the high SST and prevalent southward 700 hPa wind flow, precipitable water exhibited a moist tongue that extended poleward along the coast of Namibia (>42 mm, Fig. 3b). The 500 hPa geopotential height map (Fig. 3c) had a broad ridge south of the continent with a cut-off low feature near Cape Town (35°S, 15°E). Ahead of the cut-off low 700 hPa winds were >15 m s^{-1} (Fig. 3d) and drew tropical air poleward across the Kalahari. There was an anticyclonic circulation over Mozambique feeding the cloud band, as highlighted by the low level stream function (Fig. 3e). This feature fits neatly into the negative loaded area of Fig. 1b. At the upper level, there was notable divergence over the Kalahari according to the field of velocity potential (Fig. 3f).

Amongst factors that invigorate Kalahari cloud bands, the diurnal cycle of heating is one. To evaluate this, 0200-0800 LST fields for 5-7 April 2001 were subtracted from 1400-2000 LST fields. The results are provided in Fig. 4. Thermal differences between night and day activate an onshore westerly flow of 5 m s^{-1} at 700 hPa over the Kalahari (Fig. 4a), and vertical uplift is much enhanced during the afternoon in an elongated NW-SE axis extending over 2,000 km (Fig. 4b). A meteogram for 25ºS, 18ºE (Fig. 4c) indicates one main pulse of uplift on the sixth as winds shifted from northerly to westerly. NCEP Global Forecast System (GFS) model latent and sensible heat fluxes reached 260 and 40 W m^{-2}, respectively, while over 50 mm of rain fell mainly during the afternoon and evening of 6 April 2001.

This Kalahari cloud band case is further analyzed in Fig. 5a-d. The NCEP cloud work function (similar to convective available potential energy) highlights a narrow N-S axis of deep convection mainly over Angola (10-25°S, 15-18°E) with values >1,000 J kg^{-1} (Fig. 5a). A hovmoller plot constructed on 15-20°E over the 1-12 April period reveals the penetration of tropical moisture from 10 to 35°S during the event. Initially, the moist air is swept southward across a broad front, then as the cut-off low approaches, the moisture is drawn into a narrow band (Fig. 5b). A Hysplit back-trajectory analysis based on GFS data (Fig. 5c) indicates sources of air for northern and central points in

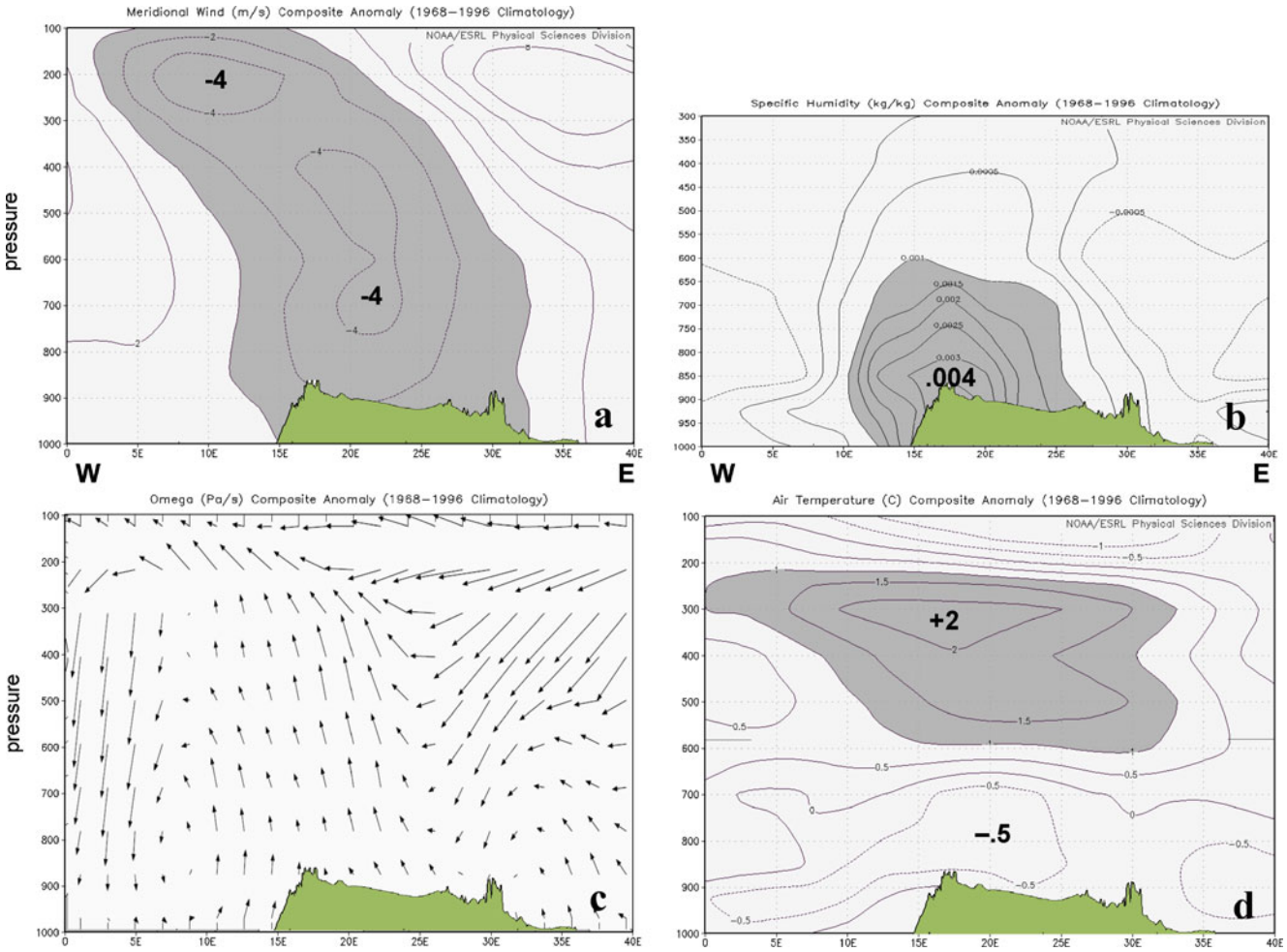

Fig. 7 Composite anomaly east-west sections along 20-25°S, of four peak cases in the 2004-2006 summers: **a** meridional wind, **b** specific humidity (kg/kg), **c** zonal wind (largest vector 20 m s^{-1}) and vertical motion (exaggerated tenfold), and **d** temperature (C) **c** with freezing level tick mark. Plateau profile is given

the cloud band from the Congo, Zambezi, and Limpopo Valleys (around Zimbabwe), hence from land with high vegetation fraction (Fig. 5d). Parcel paths describe an anticyclonic arc around the small ridge (cf Fig. 3e). Vertical trajectories exhibit gradual uplift in the days prior to the event, while on the sixth uplift is more sudden. The sources of air feeding the cloud band are moistened via evapotranspiration from surfaces to the northeast (GFS flux ~300 W m^{-2}), while high SST off Angola enhances the convective energy, providing a tropical 'anchor'.

3.3 Composite analysis of Kalahari cloud bands

Composites anomalies are constructed by averaging 3-day fields for four events in the 2004-2006 period, and subtracting the historical mean to produce maps in Fig. 6a-f. The warm SST area west of Angola is clear with temperatures >1.2 C above normal (Fig. 6a). Anomalous 700 hPa winds flow directly from warm SSTs eastward, then turn poleward around 20ºE, creating cyclonic vorticity over the Kalahari (Fig. 6b). The 500 hPa geopotential height pattern reveals a low pressure cell at 25°S, 10°E cut-off from the mid-latitudes by a high pressure anomaly at 40°S, 20°E (Fig. 6c). The satellite OLR (Fig. 6d) and precipitable water signals (Fig. 6e) reflect a NW cloud band, anomalies are<–40 W m^{-2} and >+9 mm over the Kalahari. The composite 200 hPa wind anomaly up to 14 m s^{-1} reveals a marked ridge east of South Africa forming a 'right hook' pattern (Fig. 6f).

Composite vertical sections are illustrated in Fig. 7a-d. According to NCEP reanalysis, anomalous poleward flow of 1,000 km width extended through the troposphere, tilting 1,000 km westward with height (Fig. 7a). Most of the moisture surplus is near the surface (Fig. 7b) supporting the notion that evapotranspiration is important. Upward motion is prevalent over the western plateau of southern Africa within an easterly flow (Fig. 7c), and reaches a maximum at 400 hPa causing a +2°C departure of temperature above the

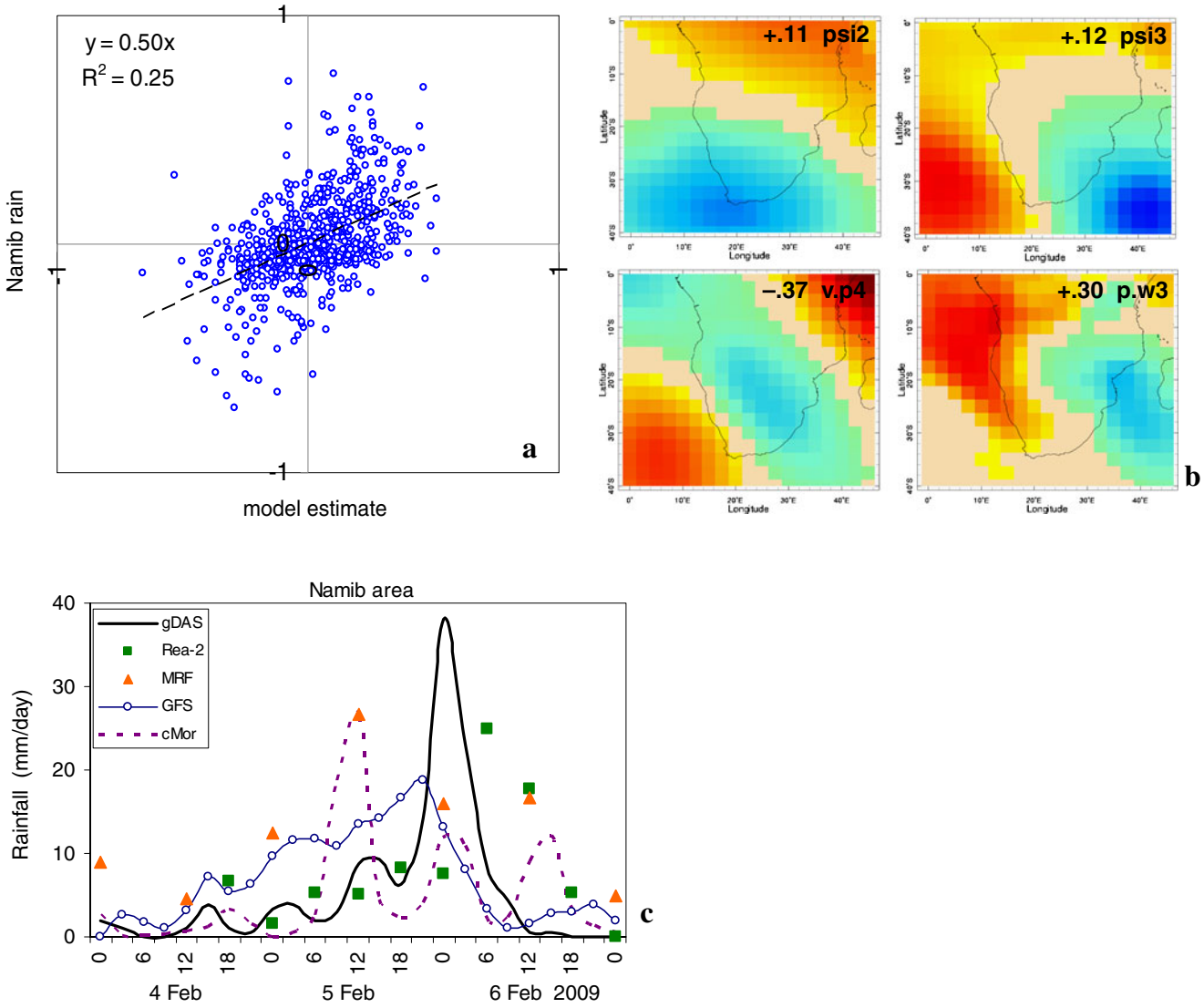

Fig. 8 **a** Scatterplot of model fitting daily rainfall with atmospheric fields: **b** (*clockwise from top left*) 850-700 stream function mode-2 and stream function-3, 850-700 velocity potential-4, and precipitable water-3; SVD loading patterns are shown at right with coefficients. Colors are *blue* −3σ to orange +3σ. **c** Comparison of MRF and GFS 2-day lead forecasts for the 2009 event with satellite (cMor), reanalysis (Rea-2) and gauge (gDAS) data, averaged over northern Namibia

freezing level (Fig. 7d). There are zones of decending motion at 5° and 30°E, forming an undulating helical overturning pattern. The system's timing (late summer), westward tilt and latent heating give it a mixed tropical-temperate character.

Radiosonde and microwave satellite profiles during these events were consulted and summarized as follows: Cloud top temperatures over Angola and Namibia were<–60°C in a 300 km wide arc where cloud liquid water exceeded 0.5 kg m^{-2}. Cloud liquid water (ice) was high at 700 hPa (200 hPa), and rain rates of 20 mm hr^{-1} produced latent heating mainly above 600 hPa. Successive radiosonde profiles at Windhoek (23ºS, 18ºE) indicated an unstable dry adiabatic lapse rate up to 500 hPa where a 2°C ~50 hPa deep capping inversion was located. Dewpoint depressions were typically ~10°C through the troposphere outside the cloud band and as a result, values of CAPE, Lifted Index, etc. were unexceptional at Windhoek. Flow below the inversion was easterly, above: northerly. As the cut-off low passed to the south, winds above 300 hPa swung to westerly and accelerated to ~30 m s^{-1}.

3.4 Forcing and prediction of Kalahari cloud bands

The environmental influences and prediction of Kalahari cloud bands are described in this section. SVD analysis was extended to daily NCEP fields found to be important in the case study analysis. Certain parameters and modes were found to have greater influence over rainfall mode-2 in step-wise multi-variate regression. The scatterplot in Fig. 8a compares 3-day observed and predicted rainfall in the

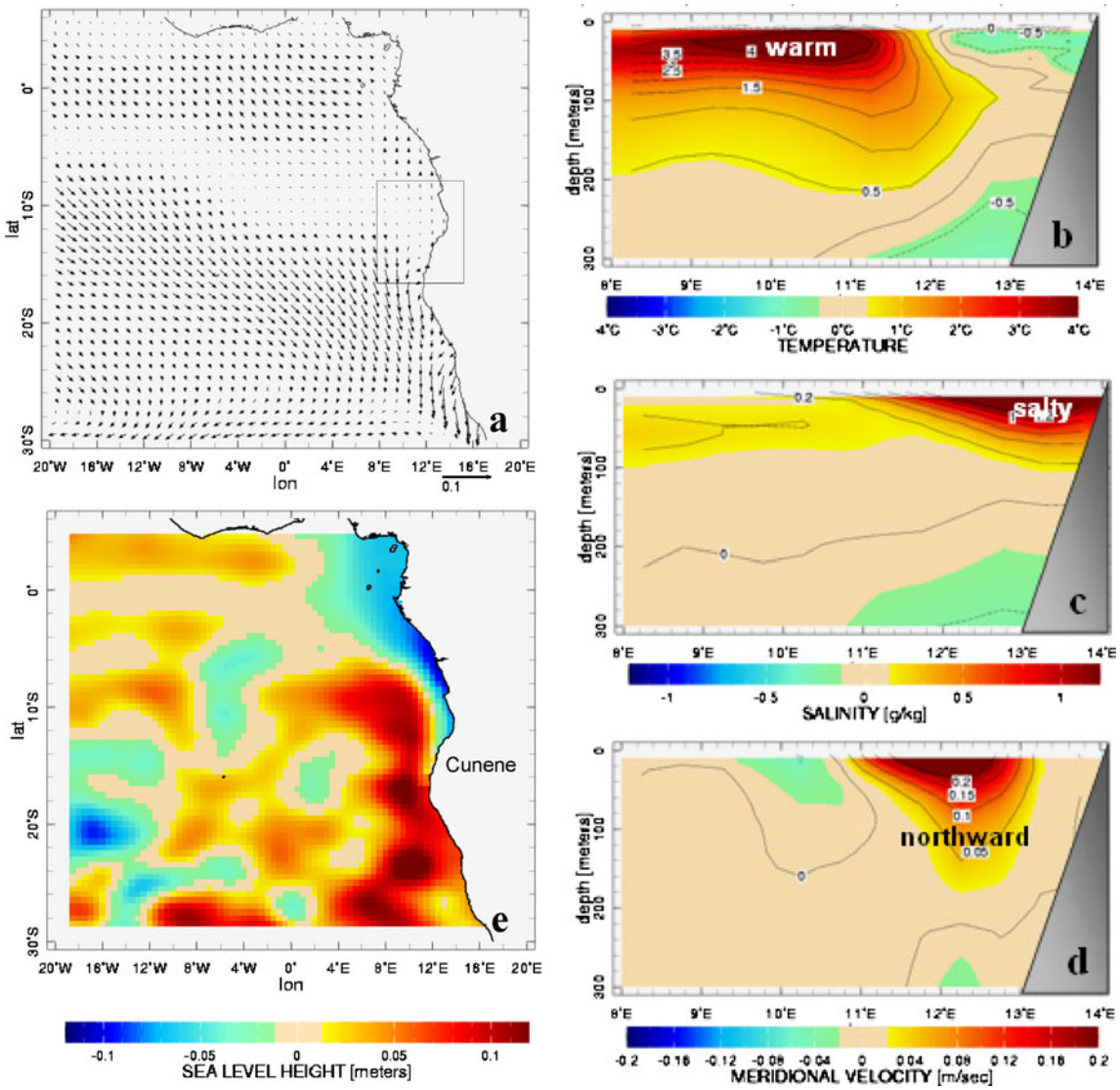

Fig. 9 Composite ocean fields for February-March seasons with warm Angola—wet Kalahari conditions minus cool dry seasons. **a** ECMWF wind stress, **b**, **c**, **d** depth sections averaged over box in **a** with coast on the right for temperature, salinity, and meridional currents, **e** sea level height

2000-2008 period and exhibits a 25% fit (N=700). Modes-2 and 3 of the low level stream function (Fig. 8b) describe anticyclonic ridging of mid-latitude flow that promotes convection over the Kalahari. In particular, psi-3 acts to shift cloud bands to the western half of southern Africa, creating the dipole noted in Fig. 1b. The low level velocity potential mode-4 pattern has greatest influence and reflects a NW-SE oriented Rossby wave similar to that simulated by Crimp et al. (1997). The alternating convergent-divergent bands suggest a helical overtuning circulation (cf. Fig. 7c). The precipitable water mode-3 pattern is consistent with the rainfall mode-2 east-west dipole: moistening over Angola-Namibia coincides with drying over Mozambique. The kinematic fields conspire to switch airflow to the Kalahari between mid-latitude and tropical sources at frequencies ~15 days, while the precipitable water contributes an annual cycle that confines Kalahari cloud bands to summer.

Data from operational numerical weather models can be used to evaluate the short-range predictability of flood events over the Kalahari. Although many cases are available for analysis; here, the destructive 2009 event is considered and intercomparisons are made for northern Namibia (17-22°S, 15-20°E). The peak rainfall (>100 mm) from gauge records occurred 1800-2400 LST 5 February (Fig. 8c). Winds were ~10 m s^{-1} easterly (westerly) in the 925-600 hPa layer over Namibia (Angola) generating cyclonic relative vorticity of -10^{-4} s^{-1}. The 2-day lead 2° resolution NCEP Medium Range Forecast (MRF) model had peak rainfall early on the fifth with amounts 30% below observed. The 0.5° resolution GFS model predicted a gradual increase of rainfall. Totals were close to observed

and the timing was 3 h early. Rainfall intensity was correctly forecast by the GFS model at lead times up to 5 days. The NCEP reanalysis-2 rainfall assimilation was reasonable, but the timing was 6 h late for the peak. The multi-satellite cMorph (Joyce et al. 2004) rainfall estimate was consistent with the MRF model, with peak values 12 h early.

The oceanographic backdrop to wet summers over the Kalahari involves a warming of SST west of Angola. Seasonal composite anomalies are plotted for the southeast Atlantic in Fig. 9 from SODA re-analyses. The most conspicuous feature is anomalous northwest wind stress that induces warming in the northern Benguela (10-25°S, 20°W−10°E) through reduced heat flux and weakened coastal upwelling. Depth sections on 12°S illustrate a warm layer (>+2°C, 20-50 m depth, 10°E) that raises sea levels offshore. An anomalous northward current is produced along the Cunene coast that entrains warm water. A salty near-shore zone develops from reduced run-off in northern Angola, as convection shifts south to the Kalahari. It is argued that the oceanic conditions that promote high rainfall in late summer also invigorate intraseasonal cloud bands. At the global scale, a cool La Niña pattern arises in the Pacific as outlined in Muller et al. (2007).

4 Conclusions

Our understanding of weather interactions over tropical Africa is growing. Here, the characteristics of flood-producing cloud bands over the Kalahari Desert have been described using daily time-scale reanalysis and satellite data, extending the earlier work of Muller et al. (2007). The cloud band stretches from Angola southward to South Africa, producing high rainfall for short spells over Namibia. The frequency of occurrence of this meridional rain mode is ~8% in the period 1996-2008. The environmental features evident from case study and composite analysis include: (1) cut-off low over the Namibian coast and high pressure ridge south of Africa, (2) inflow from vegetated surfaces of tropical Africa into a narrow meridional axis, (3) a large-scale sea breeze that enhances convection during afternoon, and in the background, (4) warming of the southeast Atlantic Ocean off Angola through reduction of upwelling favorable winds and associated heat fluxes. Composite anomalies indicate that a NW-SE oriented Rossby wave in the sub-tropical westerlies induces a cut-off low that draws tropical moisture toward the Kalahari. A large-scale sea breeze enhances convection during afternoon. Short-range GFS forecasts appear accurate for the devastating 5 February 2009 event 2-5 days in advance. Further efforts to better understand and predict these convective bands will involve extending observations and cloud-resolving mesoscale models across the region.

Acknowledgments The author thanks the many suppliers of data to enable the research.

References

Alexander WJR, van Heerden J (1991) Determination of the risk of widespread interruption of communications by floods. Department of Transport Research Project RDAC 90/16, Pretoria.

Bretherton CS, Smith C, Wallace JM (1992) An intercomparison of methods for finding coupled patterns in climate data. J Climate 5:541–560

Camberlin P, Janicot S, Poccard I (2001) Seasonality and atmospheric dynamics of the teleconnection between African rainfall and tropical sea surface temperature: Atlantic vs. ENSO. Int J Climatol 21:973–1005

Carton JA, Giese BS (2008) A reanalysis of ocean climate using Simple Ocean Data Assimilation (SODA). Mon Wea Rev 136:2999–3017

Crimp SJ, vanDenHeever SC, D'Abreton PC, Tyson PD, Mason SJ (1997) Mesoscale Modelling of tropical-temperate troughs and associated systems over Southern Africa. WRC Report 595/1/97, p 395

Dyson LL, vanHeerden J (2001) The heavy rainfall and floods over the northeastern interior of South Africa during February 2000. S Afr J Sci 97:80–86

Harrison MSJ (1988) Rainfall and precipitable water relationships over the central interior of South Africa. S Afr Geogr J 70(2):100–111

Herman A, Kumar VB, Arkin PA, Kousky JV (1997) Objectively determined 10-day African rainfall estimates created for famine early warning systems. Int J Remote Sens 18:2147–2159

Hirst AC, Hastenrath S (1983) Diagnostics of hydrometeorological anomalies in the Congo basin. Q J R Meteorol Soc 109:881–892

Huffman GJ, Adler RF, Morrissey M, Bolvin DT, Curtis S, Joyce R, McGavock B, Susskind J (2001) Global precipitation at one-degree daily resolution from multi-satellite observations. J Hydrometeor 2:36–50

Joyce RJ, Janowiak JE, Arkin PA, Xie PP (2004) cMorph: a method that produces global precipitation estimates from passive microwave and infrared data at high spatial and temporal resolution. J Hydrometeorol 5:487–503

Jury MR, Engert S (1999) Teleconnections modulating inter-annual climate variability over northern Namibia. Intl J Climatol 19:1459–1475

Jury MR, Mpeta EJ (2009) African climate variability in the satellite era, Theor Appl Climatol., doi:10.1007/s00704-009-0106-0

Jury MR, Mulenga H, Rautenbach H (2000) Tropical Atlantic variability and Indo-Pacific ENSO: statistical analysis and numerical simulation. Global Atmos Ocean System 7:107–124

Jury MR, Matari EE, Matitu M (2008) Equatorial African climate teleconnections. Theor Appl Climatol. doi:10.1007/s00704-008-0018-4

Kalnay E et al (1996) The NCEP/NCAR 40-year reanalysis project. Bull Am Meteorol Soc 77:437–471

Karoly DJ, Vincent DG (1998) Meteorology of the Southern hemisphere. Amer Meteorol Soc Boston 27 (49): p 410

Laing A, Fritsch JM (1993) Mesoscale convective complexes in Africa. Mon Weather Rev 121:2254–2263

Lindesay JA, Jury MR (1991) Atmospheric controls and characteristics of a flood event in central South Africa. Int J Clim 11:609–627

Love TB, Kumar V, Xie P, Thiaw W (2004) A 20-year daily Africa precipitation climatology using satellite and gauge data. In Proc.

84th AMS Annual Meeting, Conference on Applied Climatology P5.4, Seattle.
McCollum JR, Gruber RA, Ba MB (2000) Discrepancy between gauge and satellite estimates of rainfall over equatorial Africa. J Appl Meteoro 39:666–679
Muller A, Reason CJC, Fauchereau N (2007) Extreme rainfall in the Namib desert during late summer 2006 and influences of regional ocean variability. Intl J Climatology 28:1061–1070
Mutai CC, Ward NM (2000) East African rainfall and the tropical circulation/convection on Intraseasonal to Interannual timescales. J Climate 13:3915–3939
Rouault M, Florenchie P, Fauchereau N, Reason CJC (2003) South East Atlantic warm events and southern African rainfall. Geophys Res Lett 30: doi:10.1029/2002GL014840
Singleton AT, Reason CJC (2007) Variability in the characteristics of cut-off low pressure systems over subtropical southern Africa. Int J Climatology 27:295–310
Smith TM, Reynolds RW (2004) Improved extended reconstruction of SST (1854–1997). J Clim 17:2466–2477
Taljaard JJ (1985) Cut-off lows in the South African region. S. Afr. Weather Service Tech. Paper 14, Pretoria, p 153
Taljaard, JJ (1994) Atmospheric circulation systems, synoptic climatology and weather phenomena of South Africa. Part 1: controls of the weather and climate of South Africa. S. Afr. Weath. Service Tech. Paper 27, Pretoria, p 45
Tazalika L, Jury MR (2008) Spatial and temporal patterns of intra-seasonal rainfall oscillations over tropical Africa: their evolution and propagation. Theor Appl Climatology. doi:10.1007/s00704-007-0349-6
Todd MC, Washington R (2004) Climate variability in central equatorial Africa: influence from the Atlantic sector. Geophys Res Lett 31:23201–23205
Triegaardt, DO, vanHeerden, J and Steyn, PCL (1991) Anomalous precipitation and floods during February 1988. S. Afr. Weath. Serv. Tech. Paper 23, Pretoria, p 25
Zipser EJ (2003) Some views on hot towers after 50 years of tropical field programs and 2 years of TRMM data, in Cloud Systems, hurricanes and TRMM. Tao W-K, Adler R (eds) Monograph 51, Amer. Meteorol. Soc. Boston, pp 49–58